

## METASOMATISM AT A GRANITIC PEGMATITE – DUNITE CONTACT IN GALICIA: THE FRANQUEIRA OCCURRENCE OF CHRYSOBERYL (ALEXANDRITE), EMERALD, AND PHENAKITE

AGUSTIN MARTIN-IZARD, ANDRES PANIAGUA AND DAMASO MOREIRAS

*Departamento de Geología, Universidad de Oviedo, Arias de Velasco s/n, 33005 Oviedo, Spain*

ROGELIO D. ACEVEDO

*Cirgeo (Conicet) Ramírez de Velasco 847, 1414, Buenos Aires, Argentina*

CELIA MARCOS-PASCUAL

*Departamento de Geología, Universidad de Oviedo, Arias de Velasco s/n, 33005 Oviedo, Spain*

### ABSTRACT

The Franqueira deposit is the first documented example of a gem-quality chrysoberyl, emerald, and phenakite deposit in western Europe. It is located in the northwestern part of the Iberian Peninsula, in the Galicia – Tras os Montes zone, which is made up of two domains: (1) schistose rocks, including mafic-ultramafic overthrust complexes, and (2) granitic rocks, including peraluminous, heterogeneous, synkinematic two-mica granitic rocks. Bodies of granitic pegmatite intrude the schist and granitic rocks. At Franqueira, a pegmatite body related to the heterogeneous granites cross-cuts an ultramafic rock of dunitic character and associated gabbroic lithologies. In the contact between pegmatite and dunite, a metasomatic zone has been developed in which dunite is almost completely altered to phlogopite at the contact; distal to the pegmatite, dunite is altered to tremolite. Adjacent to the dunite, the metasomatism produced an orthoamphibole (anthophyllite-rich) rim. The phlogopite-rich metasomatic rocks contain the minerals of gemmological interest, together with apatite. All these metasomatic rocks have a high content of Mg and Cr, which come from the dunite, and of Al, K, Be, and Si, which come from the pegmatite. Three types of fluid inclusions have been distinguished. The fluid-inclusion populations of emerald and phenakite are similar. No measurable fluid-inclusions can be found in chrysoberyl. Two discontinuous hydrothermal stages have been identified. The first stage was characterized by the trapping of two types of aqueous fluid-inclusions with some volatile components. The two types of inclusions may be contemporaneous, which suggests immiscibility in the system  $H_2O - NaCl - CH_4 - CO_2$  – other volatile components. Homogenization temperatures range between 318 and 381°C. The characteristics of type-3 inclusions suggest an independent episode of fluid circulation during later tectonic events. The genetic model proposed involves emplacement of pegmatite and associated mobile elements (e.g., Be, B, P) into dunite, with subsequent metasomatism of the dunite into phlogopite and tremolite rocks near the pegmatite body. The formation of chrysoberyl is probably due to the fact that it shares structural features with the olivine; therefore, the growth of chrysoberyl could be favored by epitactic nucleation on olivine relics. Emerald is the latest Be mineral to form; it partially replaces chrysoberyl and phenakite, and could have formed by the reaction  $chrysoberyl + phenakite + quartz \rightarrow emerald$ , until quartz is exhausted.

*Keywords:* granitic pegmatite, metasomatism, dunite, emerald, chrysoberyl, “alexandrite”, phenakite, genetic model, Galicia, Spain.

### SOMMAIRE

Franqueira est le premier exemple d'un gisement à chrysobéryl, émeraude et phénakite gemmes de l'Europe occidentale. Ce gisement est situé dans la partie nord-ouest de la péninsule ibérique, dans la zone de Galice – Tras os Montes, constituée de deux domaines: (1) socle schisteux, comprenant des unités mafiques ou ultramafiques charriées, et (2) des roches granitiques, comprenant des granites hyperalumineux à deux micas, hétérogènes, et syncinématiques. Les massifs de pegmatite granitique recoupent les schistes et les roches granitiques. A Franqueira, un massif de pegmatite lié aux granites hétérogènes recoupe une dunite et un cortège de roches gabbroïques associées. Au contact entre la pegmatite et la dunite, une zone métasomatique s'est développée dans laquelle la dunite a presque complètement été transformée en phlogopite au contact avec la pegmatite; plus loin, elle est transformée en trémolite. Près de la dunite, la métasomatose a produit un liseré d'orthoamphibole de type anthophyllite. Les roches à phlogopite contiennent les minéraux d'intérêt gemmologique, accompagnés d'apatite. Toutes ces roches d'origine métasomatique contiennent des teneurs élevées en Mg et Cr, qui proviennent de la dunite, et en Al, K, Be et Si, qui proviennent de la pegmatite. Trois sortes d'inclusions fluides sont présentes. Celles qui sont piégées par l'émeraude et la

phénakite sont semblables. Le chrysobéryl ne contient aucune inclusion mesurable. Nous distinguons deux stades discontinus d'activité hydrothermale. Au cours du premier, deux types d'inclusions aqueuses ont été piégées, avec inclusions d'une phase gazeuse. Ces deux types d'inclusion auraient pu être contemporains, et témoigneraient peut-être d'un phénomène d'immiscibilité dans le système  $H_2O - NaCl - CH_4 - CO_2$  - autres composants volatils. La température d'homogénéisation s'étale entre 318 et 381°C. Les caractéristiques des inclusions du type 3 font penser qu'il y a eu un épisode indépendant de circulation de fluide lors d'événements tectoniques tardifs. Le modèle génétique propose la mise en place d'une pegmatite et d'une phase fluide associée enrichie en Be, B et P dans la dunite, avec métasomatose de la dunite, pour donner des roches à phlogopite et à tremolite près du contact. La formation du chrysobéryl serait due à la ressemblance structurale de cette espèce et de l'olivine, et à la croissance épitactique de l'un sur les reliques de l'autre. L'émeraude est plus tardive; elle remplace en partie le chrysobéryl et la phénakite, et pourrait avoir cristallisé selon la réaction chrysobéryl + phénakite + quartz → émeraude, jusqu'à l'élimination du quartz.

(Traduit par la Rédaction)

**Mots-clés:** pegmatite granitique, métasomatose, dunite, émeraude, chrysobéryl, "alexandrite", phénakite, modèle génétique, Galice, Espagne.

## INTRODUCTION

In Galicia, in the northwestern region of the Iberian Peninsula, occurrences of granitic pegmatite may contain minerals of gemmological interest. The Franqueira pegmatite is especially interesting because of its association with crystals of emerald, phenakite and chrysoberyl (variety "alexandrite"). These minerals appear where the pegmatites cross-cut dunitic rocks. The dunite directly in contact with the pegmatite is totally transformed into phlogopite, and tremolite further away. The phlogopite is of special interest, because it hosts several minerals of gemmological interest, together with apatite. This paper describes the results of a mineralogical and geochemical study of the gem-bearing rocks at Franqueira. Fluid-inclusion data are reported for emerald and phenakite. Our study establishes a genetic model that can be used as a guide for prospecting and exploration for this type of deposit.

The Franqueira ore was discovered in 1971, during construction of the Paraños-Sendín road. The first emerald crystals were recognized by a school-teacher, E. Samartino, who notified several collectors. The collectors were the first to "exploit" the ore; they took out the best crystals. Some of these crystals came to the University of Oviedo. By 1989, Franqueira was a well-known locality among collectors, but by that time, it was difficult to obtain good crystals. The number of emerald crystals extracted is unknown, but probably number a few thousand crystals of quality. The largest and the best quality is 30 × 10 cm in size and dark green in color, with good transparency. Most of the emerald crystals have good quality for cabochon, but only some have sufficient quality for faceted stones.

In 1990, a collector looking for emerald brought to our attention a mineral which was later identified as chrysoberyl, gemmological variety "alexandrite" (green under daylight and red under incandescent light). This paper is the first documentation of the Franqueira deposit, which is being mined for chrysoberyl, emerald, and phenakite ore.

## GEOLOGICAL SETTING

The Franqueira gem deposit is located in the Galicia - Tras Os Montes zone (Matte 1968), which consists of two domains, one schistose and the other granitic. The former is composed of metamorphic rocks and the Lalín-Forcarey Unit, the southern end of the large Ordenes Complex (Barrera *et al.* 1989, Monterrubio 1991). The metasedimentary rocks include mica and quartz schist, paragneiss, quartzite, calc-silicate units and metavolcanic rocks that are felsic in character. The Lalín-Forcarey Unit, as well as the Ordenes Complex, which overthrusts the other groups of the schist domain, are made up of amphibolitic gabbro, amphibolite, orthogneiss, dunite and other ultramafic rocks (Monterrubio 1991).

All of the rocks of the schist domain were affected by at least three main phases of the Hercynian Orogeny (Barrera *et al.* 1989). The first phase of the Orogeny is manifested in the region by a schistosity (S1) preserved in minerals delimited by the second-phase schistosity. No folds can be attributed to the first phase. The second phase of the Hercynian Orogeny in the Galicia - Tras Os Montes area developed a regional schistosity (S2), subhorizontal recumbent folds trending north-south, and thrust faults. During the third main phase of the orogeny, a crenulation schistosity and N-S-trending folds with a vertical axial plane were developed.

Ophiolite complexes in Galicia (Cabo Ortegal and Ordenes complexes) and Portugal (Bragança and Morais complexes) represent fragments of oceanic crust that were thrust over the schist domain during the second phase of the Hercynian Orogeny (Barrera *et al.* 1989). The study area (Fig. 1) is located between the Portuguese and Ordenes complexes.

The intensity of regional metamorphism affecting these rocks is quite variable. In the study area, metamorphic grade varies from the biotite facies with garnet to an andalusite - staurolite - sillimanite - K-feldspar facies. Furthermore, it is possible to recognize contact metamorphism (andalusite hornfels

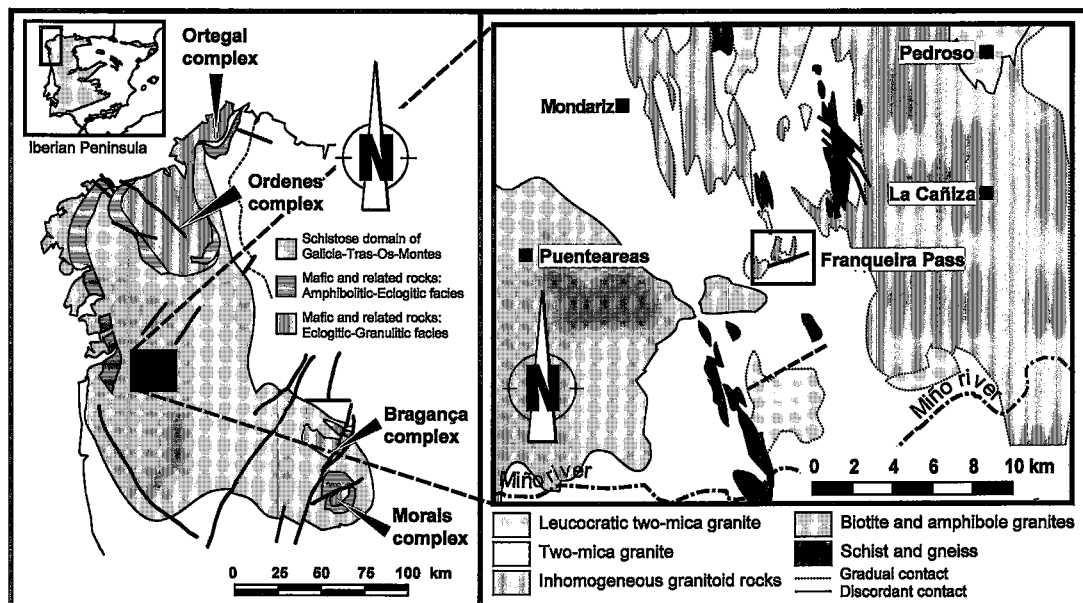


FIG. 1. Setting and schematic geological map of the Franqueira area (adapted from Barrera *et al.* 1989).

to pyroxene hornfels) caused by emplacement of igneous rocks in the host materials (Barrera *et al.* 1989).

Most of the rocks in the region are Hercynian granites. Barrera *et al.* (1989) subdivided the granites into three types on the basis of petrology and geochemistry: (1) type 1, heterogeneous two-mica granites, (2) type 2, two-mica or muscovite peraluminous granites, and (3) type 3, biotite–amphibole calc-alkaline granites. The first two types are synkinematic granites affected by the third tectonic phase (328–339 Ma), and the contacts between them are mostly gradational, but in one case (Pedroso massif), type-2 granites intruded type-1 granites. The third type of granite is postkinematic (290–310 Ma) and is intrusive in the others. The Franqueira system of pegmatite dikes is related to the synkinematic heterogeneous two-mica granites that form small outcrops in the area of Franqueira (Fig. 1). The heterogeneous granites contain abundant xenoliths and roof pendants of rocks of the schist domain, including ophiolite complexes, occasionally migmatites. Their texture and mineralogical composition is variable (Barrera *et al.* 1989). The heterogeneous granites are highly evolved (differentiation index >80), peraluminous and alkali-rich (they have more K and less Ca than type-2 granites). Contact aureoles up to 200–300 meters wide (albite–epidote hornfels) surround the heterogeneous granites and contain conspicuous large porphyroblasts of muscovite and andalusite. Pegmatite dikes are

ubiquitous and related to type-1 and -2 granites; most pegmatite bodies related to the heterogeneous granites are unzoned.

#### THE FRANQUEIRA DEPOSIT

The bodies of granitic pegmatite occur in an area located at the top of the Franqueira pass (Fig. 1), along the road from Paraños to Sendín. They form a network of narrow, anastomosing subvertical dikes that trend approximately east–west. The dike system (Fig. 2) is exposed for 15–20 meters. Dike thickness ranges from 3 to 40 cm. These pegmatite bodies are hosted by the schistose domain of Galicia – Tras Os Montes. Owing to the geometry and the nature of the contact with the host rocks, totally phlogopitized relics of schists are commonly found within the pegmatite.

The pegmatite bodies show a simple zonation, with an aplitic border. Essential minerals are quartz, albite, muscovite and scarce K-feldspar, with apatite, tourmaline and zircon as accessory minerals. The main zone of the pegmatite consists of larger crystals than those of the border, although its mineral constituents are similar. However, the relative proportions of the minerals are different. In the main zone, albite is the most abundant mineral, with quartz in lesser proportion, and some muscovite. Within the pegmatitic bodies of greater thickness, a banding can be observed in the central zone, in which a coarse-grained rock alternates with another of saccharoidal appearance. In

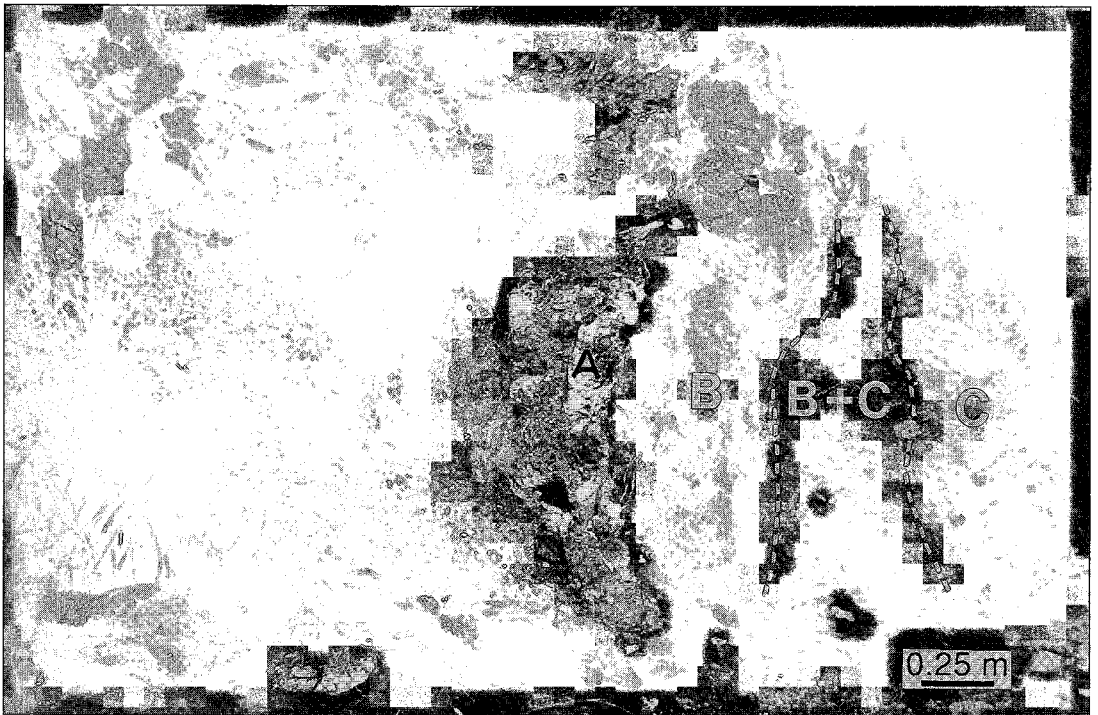


FIG. 2. View of the pegmatite dikes with lenticular geometry (A). The pegmatite is hosted by phlogopite (B) and tremolite (C).

the coarse-grained material, there are lamellar crystals of "cleavelandite" with subhedral individuals of albite, interstitial euhedral quartz, and muscovite plates. In the saccharoidal facies, garnet and tourmaline abound. Other accessory minerals are zircon, fluorapatite, pyrite, ilmenite and pyrrhotite, all of which are anhedral. All these minerals have been tectonized, as shown by the curved plagioclase twins, wavy extinction in quartz, and kinked flakes of flexured mica. The plagioclase is partially sericitized, mostly near the phlogopite.

Owing to the peculiar geometry of the pegmatite bodies, their irregular edges and imprecise contacts with the country rocks, the presence of xenoliths, and the coarse-grained nature of these rocks, samples selected for a geochemical study are not totally representative, as in all cases they are partially contaminated by the host. Results of whole-rock chemical analyses are shown in Table 1. The pegmatite has Si, Al and alkali contents that are normal for this type of rock; the high values for Mg and Fe are attributed to the above-mentioned contamination.

The host rocks have a sharp contact with the pegmatites and are of a micaceous nature. The mica is phlogopite, and it is the most abundant mineral in this

TABLE 1. REPRESENTATIVE WHOLE-ROCK COMPOSITIONS, FRANQUEIRA SUITE

ROCKS	Pegmatite	Phlogopite	Tremolite	Altered Marum* Dunite	Marum* Dunite	Gabbro
wt %						
SiO <sub>2</sub>	74.80	44.18	56.97	48.22	39.8	47.26
Al <sub>2</sub> O <sub>3</sub>	14.48	14.99	4.76	3.07	0.04	21.75
Fe <sub>2</sub> O <sub>3</sub>	0.54	9.31	4.86	8.68	7.24	12.57
MgO	0.11	18.28	18.38	30.88	49.93	1.14
CaO	0.33	0.04	10.61	3.61	0.05	12.15
Na <sub>2</sub> O	5.58	0.28	0.25	1.11	0.00	0.57
K <sub>2</sub> O	1.84	10.27	2.03	1.33	0.00	0.52
TiO <sub>2</sub>	0.01	0.44	0.32	0.12	0.00	0.52
MnO	0.44	0.09	0.10	0.12	0.11	0.24
P <sub>2</sub> O <sub>5</sub>	0.12	0.07	0.04	0.06	0.00	0.21
Cr <sub>2</sub> O <sub>3</sub>	0.00	0.21	0.41	0.36	0.42	0.01
LOI	1.80	1.40	1.10	2.20	2.52	1.90
Total	99.95	99.79	99.88	99.77	100.11	99.95
ppm						
As	5	151	6	1220	no data	10
Ni	10	500	353	1547	2520	12
Cu	2	29	3	4	4	24
Co	5	49	12	69	no data	5
Be	18	9	6	4	no data	20
Li	247	568	173	22	no data	49
Ba	135	1288	161	34	no data	159
Sr	32	41	66	29	0.00	434
La	16	6	19	2	no data	81
Zr	10	21	29	5	no data	396
Y	5	5	5	5	no data	120

Total Iron as Fe<sub>2</sub>O<sub>3</sub>.

\*Chemical composition of Dunite from the Marum Ophiolite (in Middlemost 1985) for comparison with Franqueira altered dunite.

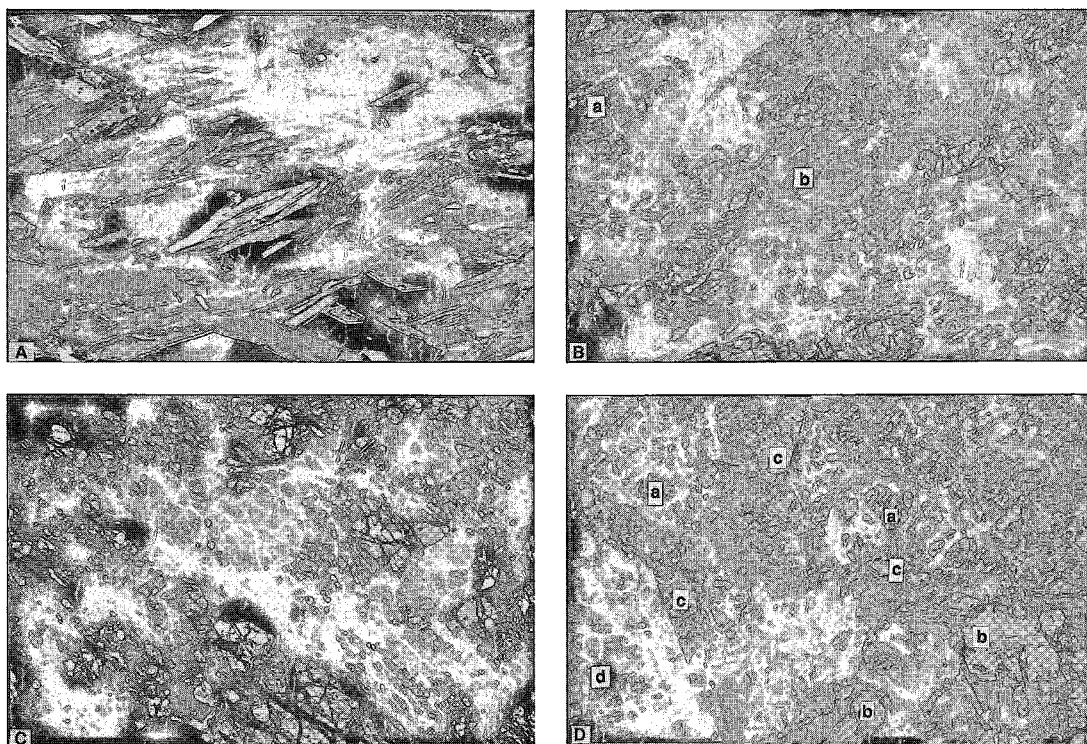


FIG. 3. A: Microscopic view of phlogopite rock. Crossed polarizers, 25 $\times$ . B: Microscopic view of tremolite rock. The amphibole (a) is intergrowth with phlogopite (b) Crossed polarizers, 35 $\times$ . C: Microscopic view of partially altered (serpentinized and chloritized) dunite rock. Crossed polarizers, 35 $\times$ . D: Microscopic view of chrysoberyl (alexandrite) (a), phenakite (b), emerald (c), and apatite (d). Phenakite and skeletal corroded crystals of chrysoberyl are included in emerald.

facies (over 75%, up to 90%) (Fig. 3A). The visible thickness of this rock is up to 3 meters and crops out for at least 5 meters. The rock has a markedly lepidoblastic texture, locally banded and crenulated. Where it contains amphibole, its texture is, in part, nematoblastic. The accessory minerals are chrysoberyl ("alexandrite"), phenakite, beryl (emerald) (Table 2), tourmaline, garnet (mainly almandine), apatite (fluorapatite, 3.5 wt.% F) and zircon. No quartz has been detected, except in one beryl crystal (we have analyzed more than 20) in which two small inclusions (10 and 20  $\mu\text{m}$ ) of quartz and one of orthoamphibole were found. The rock is partially chloritized.

Chrysoberyl [Figs. 4A, 3D(a)] appears as subhedral porphyroblasts isolated in the phlogopite, or as skeletal intergrowths with emerald, phenakite and apatite. In every case where chrysoberyl and phenakite are found together, they are replaced by beryl and appear as a skeletal intergrowth with the emerald. The twinned porphyroblasts, in size up to 1 cm across (Fig. 4A), show the pronounced pleochroism and color change (reddish color in light from an incandescent lamp, greenish color in daylight) typical of the "alexandrite"

variety. Its average Cr content is 0.29 wt.%  $\text{Cr}_2\text{O}_3$  (five crystals). Phenakite [Figs. 4C, 3D(b)] appears as subhedral and colorless prismatic crystals up to 3 cm in size. Phenakite is commonly associated with apatite crystals [Fig. 3D(d)], and also appears with chrysoberyl and emerald. Beryl appears as euhedral prismatic crystals up to 30 cm [Fig. 3D(c)] across; their intense green color and high Cr content (up to 0.2 wt.%; average, 0.11 wt.%  $\text{Cr}_2\text{O}_3$  in 11 crystals, Table 2) give it its emerald-like character. It is the latest Be mineral and replaces the chrysoberyl and phenakite (Fig. 3D). Tourmaline is developed in the contact between phlogopite and the pegmatite. All these minerals contain solid inclusions, mainly phlogopite scales.

The widespread development and extensive outcrops of the phlogopite enabled us to obtain representative samples of this particular rock-type for geochemical analysis (Table 1). The major-element whole-rock composition corresponds to nearly pure phlogopite. Concentrations of Cr (0.21 wt.%  $\text{Cr}_2\text{O}_3$ ) and other trace elements, such as Ba, Li, Ni and As, are relatively high.

TABLE 2. SELECTED RESULTS OF ELECTRON-MICROPROBE ANALYSES, MINERALS OF THE FRANQUEIRA DEPOSIT

Minerals	Oi	Chr	Phl <sup>1</sup>	Phl <sup>2</sup>	Phl <sup>3</sup>	Tr <sup>1</sup>	Tr <sup>3</sup>	Hbl <sup>4</sup>	Chy	Em	Pk	Tur <sup>core</sup>	Tur <sup>med</sup>	Tur <sup>rim</sup>	Fs	An	Grt	Chu	Ath
(N,n)	8,4	20,7	10,5	8,4	10,5	10,5	8,4	11,5	9,5	15,11	9,5	3,1	2,1	4,1	4,3	4,2	16,8	22,10	1,1
SiO <sub>2</sub>	40.82	0.01	41.58	42.53	41.09	56.37	54.35	40.61	0	67.02	54.71	37.50	37.38	37.55	51.65	44.04	36.72	36.44	63.92
TiO <sub>2</sub>	0.10	0.81	0.44	0.40	0.67	0.15	0.06	0.65	0	0	0	0.12	0.27	0.48	0.21	0.02	0.03	3.32	0.01
Al <sub>2</sub> O <sub>3</sub>	0	7.73	12.34	12.70	14.13	2.00	2.85	11.63	80.03	16.71	0	31.50	30.07	30.53	0.80	34.64	20.12	0	0.03
Cr <sub>2</sub> O <sub>3</sub>	0	55.50	0.70	0.71	0.13	0.43	0.15	0.02	0.29	0.11	0	0.05	0.19	0.29	0.04	0	0.02	0.05	0
Fe <sub>2</sub> O <sub>3</sub> **	0	4.52	0	0	0	2.17	4.52	5.61	0	0	0	0	0	0	0	0	2.27	0	0
FeO	13.11	29.67	3.60	4.43	8.33	0.54	3.86	22.86	0.75	0.71	0.02	4.61	4.27	3.77	28.7	0.4	25.79	11.99	1.48
MnO	0.15	0.45	0.03	0.04	0.11	0.07	0.55	0.20	0	0	0	0.06	0.05	0.06	0.84	0	1.45	0.19	0.02
NiO	0.08	0.03	0	0	0	0	0	0	0	0	0	0.12	0.04	0.02	0.04	0	0	0.07	0.11
MgO	47.31	2.81	26.19	24.23	20.65	22.87	19.17	2.90	0	1.07	0	9.15	10.35	10.44	13.9	0.02	0.34	46.19	30.46
CaO	0.02	0.01	0.04	0.05	0.03	13.41	12.68	11.58	0	0	0	0.89	1.93	1.99	1.01	19.24	13.06	0.01	0.05
Na <sub>2</sub> O	0.01	0	0.06	0.13	0.26	0.36	0.45	0.66	0	1.07	0.02	2.17	1.87	1.72	0.02	0.77	0	0.01	0.09
K <sub>2</sub> O	0	0	9.16	9.30	9.04	0.06	0.15	0.70	0	0.12	0	0.02	0.02	0.02	0.02	0.01	0	0.01	0
BeO**	0	0	0	0	0	0	0	0	18.88	13.23	45.30	0	0	0	0	0	0	0	0
H <sub>2</sub> O**	0	0	4.28	4.28	4.21	2.20	2.16	1.91	0	0	0	13.81	13.55	13.11	0.02	0	0	0	0
Total	101.5	101.5	98.43	98.79	98.64	100.6	100.9	99.32	99.94	100.0	100.0	100.0	100.0	100.0	97.21	99.14	99.81	98.28	96.17

Symbols for rock forming minerals are after Kretz (1983). Oi, olivine; Chr, chromite; Phl, phlogopite; Tr, tremolite; Hbl, hornblende; Chy, chrysoberyl; Em, emerald; Phe, phenakite; Tur, tourmaline; Fs, ferrosillite; An, anorthite; Grt, garnet; Chu, clinohumite; Ath, anthophyllite

<sup>1</sup> In dunite. <sup>2</sup> In tremolite. <sup>3</sup> in phlogopite. <sup>4</sup> in gabbro.

\*N: number of points analysed. n: number of crystals analysed.

\*\*Calculated by stoichiometry.

The minerals previously described have been analyzed using an electron microprobe (Table 2). Phlogopite from phlogopitite contain 20.65 wt.% MgO and 0.13 wt.% Cr<sub>2</sub>O<sub>3</sub>. In tremolite and dunite, there are also phlogopite scales with a high content of Mg

and Cr (Table 2). In thin section, the tourmaline is seen to be zoned. Microprobe analyses indicates that the tourmaline is dravite; Ti, Cr, Mg and Ca increase from core to rim (Table 2).

The phlogopitite grades into tremolite, in which

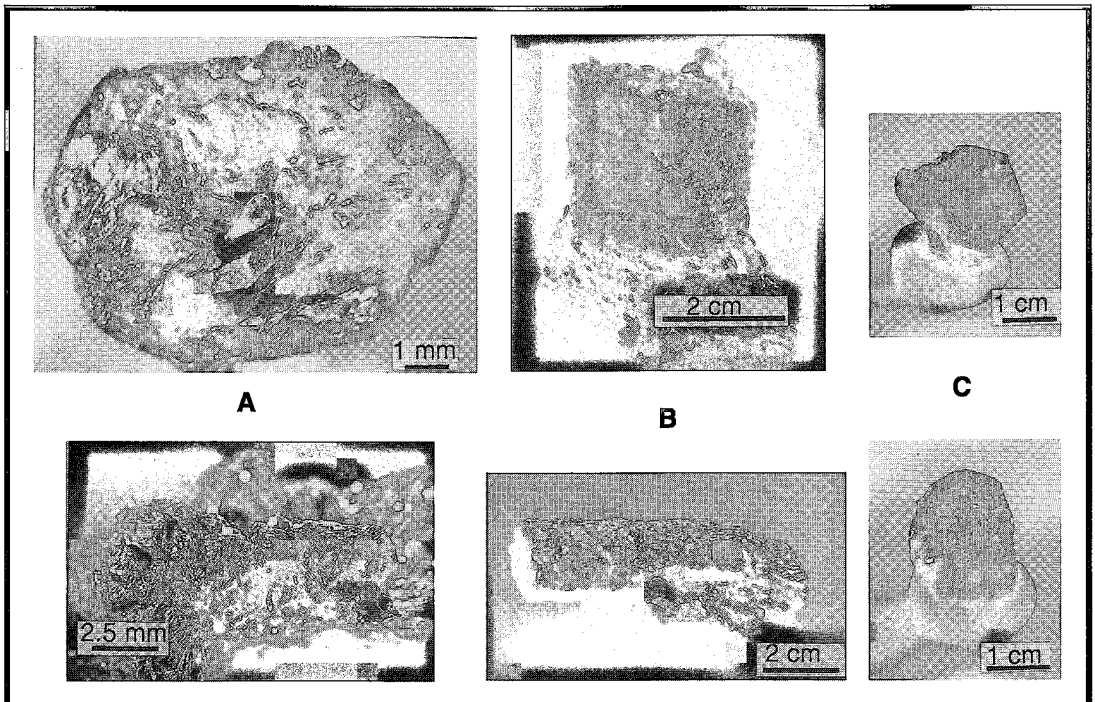


FIG. 4. (A) Twinned chrysoberyl (alexandrite) crystal. (B) Emerald crystal on phlogopite. (C) Phenakite crystal on phlogopite.

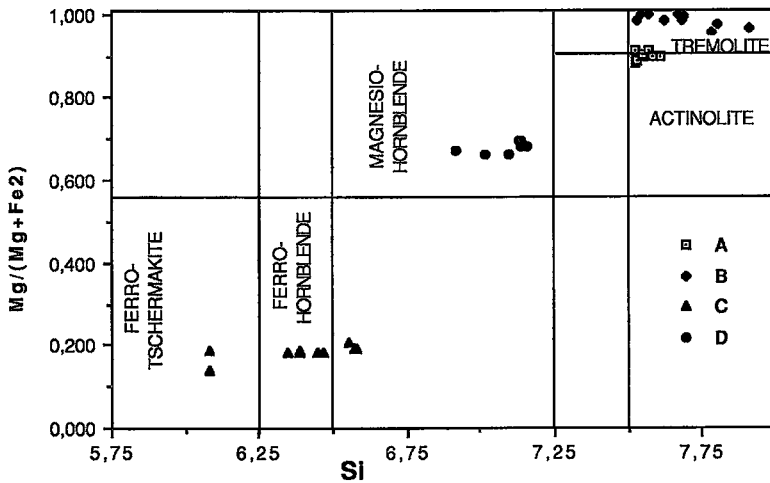


Fig. 5. Plot of the  $Mg/(Mg + Fe^{2+})$  value versus Si in calcic amphibole (adapted from Leake 1978) for the different types of amphiboles at Franqueira. Host rocks are as follows: A: phlogopite. B: dunite. C: metasomatized gabbro. D: gabbro.

pockets of phlogopite are ubiquitous. In the tremolite, the rock is essentially composed of tremolite and has a nematoblastic texture. Some phlogopite is invariably present and locally, along dunite contacts, the tremolite is rimmed by anthophyllite (Table 2) and titanite. This rock unit is at least 6 meters thick.

The amphibole grains are subhedral and partially altered to phlogopite and zoisite. Accessory minerals include zircon, apatite and ilmenite. The rock is partly altered to chlorite. Over a short distance (5 cm), the tremolite grades into an anthophyllite zone into dunite. The major-element composition of the tremolite (Table 1) corresponds to that of nearly pure tremolite, except for Fe and K, due to the presence of some phlogopite. Relatively high concentrations of Cr (0.41 wt.%  $Cr_2O_3$ ) and Ni (353 ppm) are observed.

Two populations of tremolite are observed in the tremolite (Table 2, Fig. 5); one is more magnesian, and the other one is more ferrous. In turn, the content of Cr is greater in the magnesian variant. The latter crystals are located near the dunitic rocks, whereas the ferrous variety is closer to the pegmatites.

The dunite outcrops only as relics about 1 meter across in the tremolite rock. It has a dark color, is granoblastic and has a very compact texture, and the olivine is partially altered to tremolite and phlogopite. This rock is composed chiefly of olivine; therefore, it is considered dunite. Olivine ( $Fo_{86.6}$ ) forms a hypidiomorphic, partially serpentinized and chloritized aggregate. In serpentinized areas, some individual grains are partially replaced by titanian clinohumite. Chromite is found as an accessory mineral, usually disseminated, although occasionally forming small

aggregates. There are also sulfides, generally filling cavities: nickeline, maucherite and pyrrhotite, with small quantities of pentlandite, westerveldite, millerite and chalcopyrite.

The dunite (Table 1) has an unusual chemical composition. The relatively high concentrations of silica, alumina, and alkalis in the dunite reflect partial alteration. It contains over 33 wt.% MgO, which reflects its olivine-rich composition. As for trace elements, the high contents of As, Ni and Co in this rock stand out. The concentrations of Cr and Ni in the rock are around 0.13 wt.%. The ratios of Ni/Cu (>50) and Ni/Co (>10), are very high. The concentrations of As also are high, and resemble those of Ni and Cr (0.13 wt.%). The alkalis or  $SiO_2$  content versus ferromagnesian content of the dunite and pegmatite represents end members in a sequence in which phlogopite and tremolite are intermediates.

The relatively Fe-rich nature of both olivine and chromite in the dunite (Table 2) probably reflect re-equilibration during Hercynian metamorphism. In terms of mg# and MnO content, the olivine at Franqueira is distinctly less magnesian than mantle olivine and overlaps olivine from alpine ophiolites (Fig. 6).

The compositional characteristics of the spinel grains analyzed with the microprobe agree well with those from the Moeche mafic suite [Cabo Ortegal Ophiolitic Complex: Monterrubio (1991)]. As with spinel compositions from other mafic complexes in the Hercynian Orogen of the Iberian Peninsula (Herbeira, Ordoñez and Badajoz), they plot in the field of residual peridotite and ophiolitic rocks, as defined by Jan &

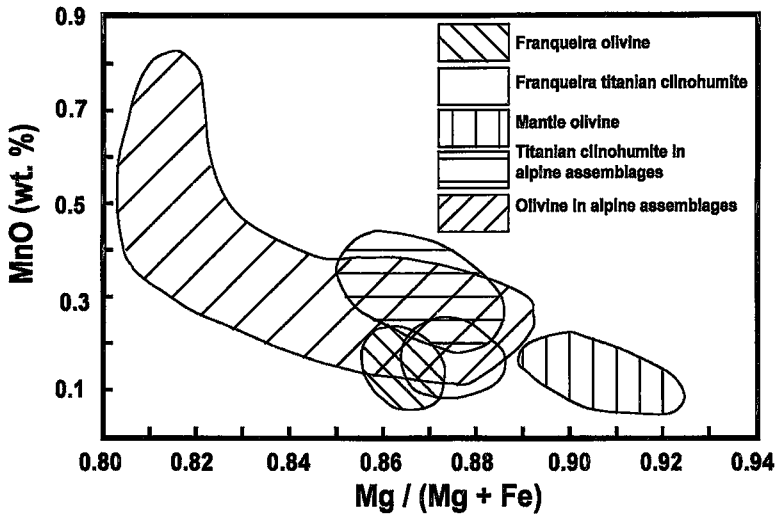


FIG. 6. Diagram from Scambelluri *et al.* (1991) and projection on their graph of Franqueira olivine and titanian clinohumite. Note that both minerals have less Mn, but the same Mg and Fe relationship, as the minerals from Alpine ophiolites. Mantle olivine shows very different values.

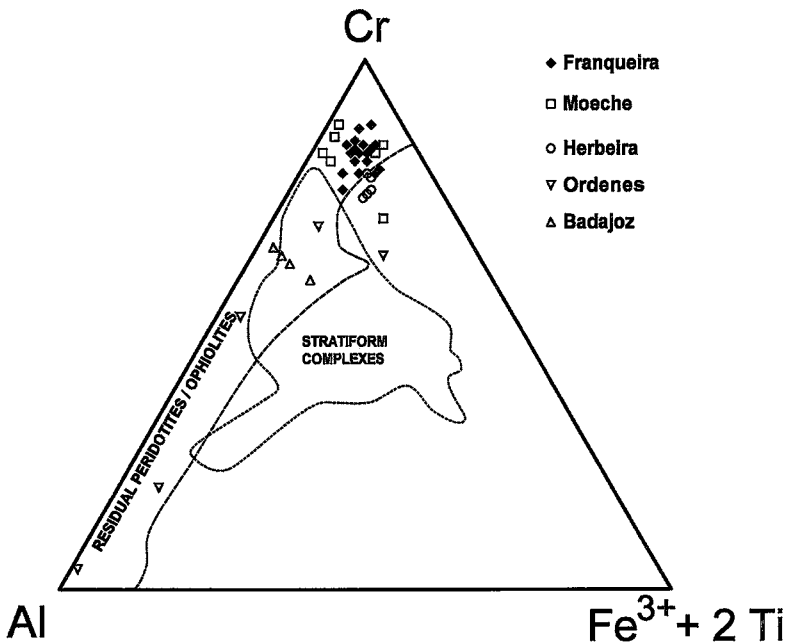


FIG. 7. Diagram from Jan & Windley (1990) showing the projection of spinel compositions from Franqueira (this study) and Herbeira, Moeche, Badajoz, and Ordenes (Monterrubio 1991). Most of the data project in the field of residual peridotite and ophiolitic rocks.

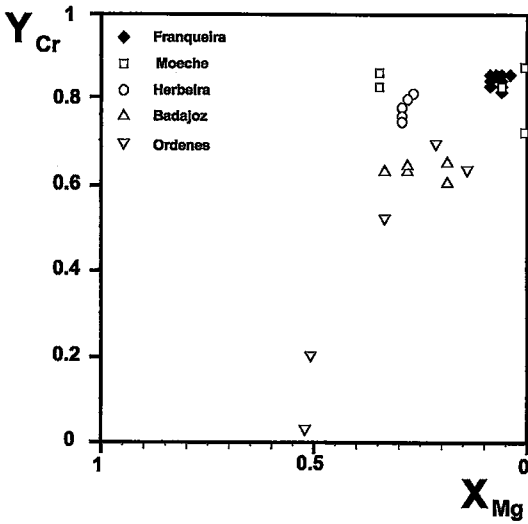


FIG. 8. Plot of  $Y_{Cr}^{pl} - X_{Mg}^{sp}$  for the chromite-bearing ultramafic ophiolitic rocks of the Variscan Massif. Symbols as in Fig. 7.

Windley (1990) (Fig. 7) and  $X_{Mg}^{sp} (= Mg/\Sigma R^{2+}) - Y_{Cr}^{pl} (= Cr/\Sigma R^{3+})$  (Fig. 8). Nevertheless, the spinel at Franqueira is Cr-rich relative to spinel in the other complexes.

The chemical composition of titanian clinohumite from Franqueira is close to the theoretical composition of this mineral. The titanian clinohumite at Franqueira (Figs. 6, 9) corresponds to that found in alpine peridotites. It can be deduced from the microscopic study that its formation is, possibly, simultaneous with that of the serpentine replacing olivine.

The phlogopite present in the dunite is richer in Mg and Cr than phlogopite from phlogopitite and tremolite. The results of electron-microprobe analyses allow us to distinguish three types of phlogopite, which in turn correspond to specific stages within the petrological sequence. The phlogopite present in the dunite is the richest in Mg (26.19 wt.% MgO) and Cr (0.7 wt.% Cr<sub>2</sub>O<sub>3</sub>); phlogopite related to tremolite is somewhat poorer in Mg (24.23 wt.% MgO), with practically the same content in Cr. Phlogopite located near the pegmatite body has a lower Mg content (20.65 wt.% MgO) and Cr (0.13 wt.% Cr<sub>2</sub>O<sub>3</sub>). Beryl, chrysoberyl and phenakite of gemmological interest appear in the last facies.

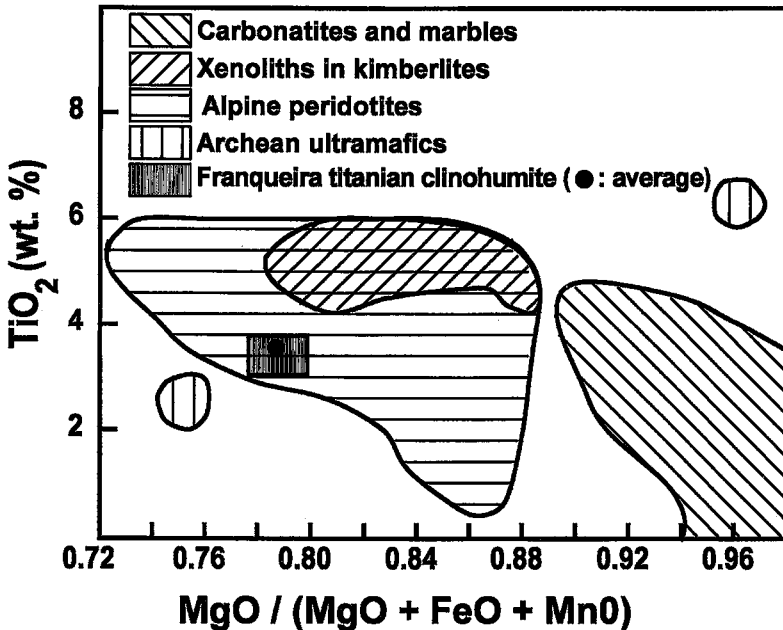


FIG. 9. Diagram adapted from Gaspar (1992) showing the composition of titanian clinohumite samples from Franqueira.

Several outcrops of amphibolitized gabbro resemble the dunite because of a dark color and granoblastic texture where it occurs between the phlogopite and tremolite. The gabbro is possibly related from a genetic point of view to the dunite, as a rock of the ophiolitic sequence. On the basis of contrasting mineralogical compositions, the metasomatism affecting the gabbro is believed to differ from the metasomatism affecting the dunite.

The gabbro is composed of calcic amphibole (Mg-rich hornblende, Fig. 5), and plagioclase ( $An_{92.2}$ ), which appears either intergrown with the amphibole or as part of a mosaic, with ferrosilite and quartz. Accessory minerals include ilmenite, rutile and zircon. This igneous rock is cross-cut by granitic pegmatite, which produced in it a second association consisting of calciferous amphiboles (tschermakite and iron-rich hornblendes, Fig. 5), with almandine, zoisite, titanite and albite.

Partially metasomatized amphibolitized gabbro (Table 1) may be slightly contaminated by phlogopite and tremolite, but because the rock is fine to medium grained, we believe our whole-rock data are representative. The hornblende gabbro is poor in Si, rich in Al, Fe, Ca and P, and poor in alkalis. Trace elements such as Y, Zr, La and Sr show anomalously high concentrations. Inclusions of zircon in hornblende produce pleochroic halos. In the gabbro, the most common alteration is phlogopitization and biotitization.

From the chemical composition of the amphiboles (Table 2), two large groups have been distinguished: orthoamphibole, corresponding to anthophyllite, and two types of clinoamphibole. In both associations, amphibolitized gabbro and metasomatized gabbro, the more abundant minerals are the clinoamphiboles. All belong to the hornblendes (magnesian, ferrous, tschermakitic and pargasitic, Fig. 5), Mg-rich hornblende in the gabbro and Fe-rich in metasomatized gabbro.

Finally, in the hornblende gabbro facies, other mineral phases coexist with the hornblende, such as tourmaline (dravite), garnet (Alm 57.8%, Grs 30.6%, Sps 3.3%, Adr 6.9%, Prp 1.4%, uvarovite 0.06%), anorthite ( $An_{93.2}$ ) and ferrosilite, the composition of which is shown in Table 1.

#### SIMILAR DEPOSITS IN THE WORLD

Formation of emerald ores requires special geological conditions to bring chromium and beryllium together. On the basis of this fact, Snee & Kazmi (1989) proposed that emerald ores will appear in three geological settings: (1) suture zones, (2) granite-greenstone terranes and (3) shale/metashale associations.

Of the emerald deposits of interest in which the same mineral association appears, the most outstanding examples are Tokovaya (Urals, Russia), described in

Sinkankas (1989) and Laznicka (1985), and the Habachtal deposit (Austria) (Sinkankas 1989), both of suture-zone type. The emerald deposits of Brazil described by Giuliani *et al.* (1990) and Souza *et al.* (1992), and the ones in Zimbabwe with the same paragenesis, and in Tanzania, without phenakite (Sinkankas 1989), belong to the granite-greenstone type (Snee & Kazmi 1989).

The Russian emerald - chrysoberyl - phenakite district, which shares the same geological setting as Franqueira, consists of three zones: the Western zone is composed of granites; the Central zone contains serpentine, phlogopite and tremolite, in which small lenticular bodies of peridotite are included. This zone contains the emerald. The Eastern zone is composed of basic and ultrabasic rocks. According to Fersman (1929), the formation of the Central zone is the result of the pinching and compression of the rocks between the granites of the Western zone and the basic and ultrabasic rocks of the Eastern zone. The formation of new minerals is due to the contribution from both to the Central zone, especially a pegmatite intrusion from the granites of the Western zone. The subsequent chemical activity altered these rocks and, owing to the introduction of a broad variety of new components (among them, rare elements), caused the formation of up to 80 mineral species. It is here that chrysoberyl (alexandrite) and phenakite were described for the first time. According to Vlasov & Kutakova (1960), emerald is found in phlogopite-rich zones (phlogopite).

#### FLUID-INCLUSION STUDIES

The study of fluid inclusions in emerald and phenakite has the potential to provide valuable information on the conditions of metasomatism around the pegmatite. Fluid inclusions in chrysoberyl are scarce, and where observed, are too small (less than 1  $\mu\text{m}$ ) for study.

Emerald and phenakite have a significant number of inclusions isolated or in groups; these are interpreted as being primary. Other inclusions related to fractures are classified as pseudosecondary or secondary, on the basis of criteria of Roedder (1984). Inclusion morphology is equally variable, being rounded, elongate, tubular, subhedral negative crystal or irregular. The size of the inclusions studied ranges from 5 to 60  $\mu\text{m}$  across (Fig. 10).

One hundred and twenty-five fluid inclusions have been selected and studied in the two minerals. In all emerald and phenakite crystals studied (more than 10), fluid inclusions have the same morphological characteristics and volumetric relations.

Three types of inclusions have been identified (Figs. 10A, B): Type-1 inclusions: Complex  $\text{CH}_4$ -bearing aqueous inclusions ( $\text{H}_2\text{O}$ -NaCl- $\text{CH}_4$  and other volatiles). These show two phases (mainly  $\text{H}_2\text{O}$  L and

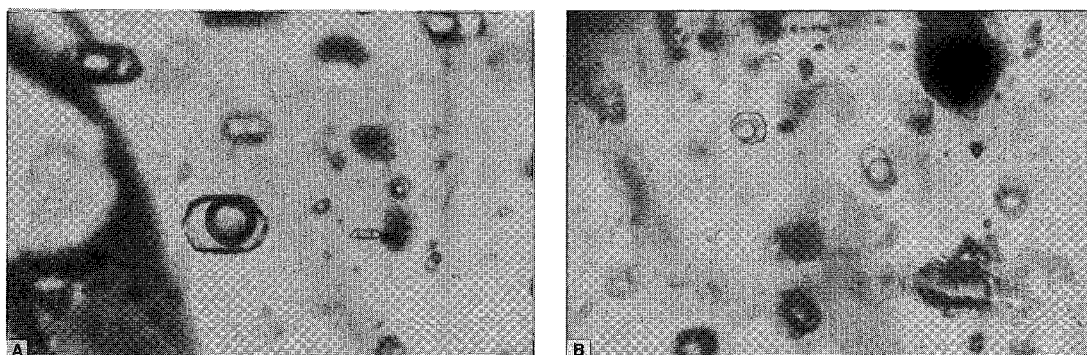


FIG. 10. A: Complex CO<sub>2</sub> aqueous inclusions (type 2) in emerald crystals. Crossed polarizers, 45 $\times$ . B: Complex CH<sub>4</sub> aqueous inclusions (type 1) in emerald crystals. Crossed polarizers, 45 $\times$ .

CH<sub>4</sub> V) at room temperature. The vapor phase occupies between 20 and 50% of the total volume of the inclusions (Fig. 10A). These inclusions, the most representative of the emerald and phenakite, are found distributed in groups, isolated or in microfractures. We consider them as primary or pseudosecondary inclusions. Type-2 inclusions: Complex CO<sub>2</sub>-bearing aqueous inclusions (H<sub>2</sub>O-NaCl-CO<sub>2</sub> and other volatiles). These inclusions contain two phases (mainly H<sub>2</sub>O L and CO<sub>2</sub> V) at room temperature and show volumetric proportions Vg/Vt (vapor volume/total volume) below 50% (Fig. 10B). These inclusions appear only in the core of emerald crystals and have the same distribution as the Type-1 inclusions, but are less abundant. Type-3 inclusions: Mixed-salt aqueous inclusions (H<sub>2</sub>O-NaCl and other salts). These show two phases (H<sub>2</sub>O L + H<sub>2</sub>O V) at room temperature in which the vapor bubble occupies less than 10%. These inclusions are found in the two minerals and are relatively scarce and secondary in character.

On each fracture, the inclusions have similar volumetric ratios and chemical compositions, suggesting that the almost continuous fracturing was accompanied by an evolution in the nature of the mineralizing fluids.

However, the inclusions that occur in clusters within the core of the emerald may correspond to the type-1 or type-2 inclusions. Some inclusions show necking-down and evidence of leakage, and so were not analyzed, since they could give anomalous microthermometric results. Volumetric ratios are constant except where altered by these processes.

The inclusions commonly contain crystalline solids, interpreted to be trapped mechanically at the moment of inclusion formation. The number and size of these solids are variable, in such a way that the ratio of volume of solids to total volume can reach 30%. The crystals are hexagonal, prismatic or completely anhedral, being transparent, colorless, and at times birefringent. They may correspond to phlogopite, emerald or phenakite, among others. The variable ratios of the volume of such solids to the volume of the fluid phase, together with the fact that some of the inclusions contain no solid at all, suggest that the crystals are not true daughters but were accidentally trapped.

The microthermometric results are summarized in Table 3, and the behavior of the fluid inclusions during heating-freezing experiments is described below.

TABLE 3. MICROTHERMOMETRIC RESULTS ON EMERALD AND PHENAKITE SAMPLES

samples	type	N <sup>o</sup>	TmCO <sub>2</sub>	TmICE	TmHyd	ThCO <sub>2</sub>	ThCH <sub>4</sub>	Th
Emerald	1	39	—	-3 to -5.2	11.5 to 19	—	-82 to -90 L -83 to -106 G	318 to 369 L 354 G 320 to 378 L
Emerald	2	31	-60.8 to -62.1	-3 to -7	11.9 to 22	-11.2 to 10G	—	381 G 381 C
Emerald	3	7	—	-1.3 to -23	—	—	—	160 to 245 L
Phenakite	1	40	—	-3.5 to -5.2	14.8 to 18.3	—	-88.6 to -109 L -86 to -106 G -86.7 to -89 C	322 to 350 L 363 to 373 G
Phenakite	3	8	—	-2.1 to -11	—	—	—	193 to 265 L

Tm: melting temperature. Th: homogenization temperature. L: liquid. G: gas. C: critical.

*Type-1 inclusions*

These inclusions were cooled to  $\sim -170^\circ\text{C}$ . After cooling and on warming, the  $\text{CH}_4$  liquid and vapor phases homogenized either into the vapor (V), liquid (L) state or with critical (C) behavior at temperatures ranging from  $-83$  to  $-106^\circ\text{C}$  into V and from  $-82$  to  $-90^\circ\text{C}$  into L phases in the emerald, and from  $-86$  to  $-106^\circ\text{C}$  into V,  $-88.5$  to  $-110.5^\circ\text{C}$  into L, and  $-86.5$  and  $-89^\circ\text{C}$  into C phases in the phenakite. In general, all inclusions homogenized (Th  $\text{CH}_4$ ) at temperatures below the critical temperature of  $\text{CH}_4$  ( $-82.1^\circ\text{C}$ , Burruss 1981). As a significant number of inclusions (7) found in phenakite have critical temperatures of homogenization slightly lower than the critical temperature of  $\text{CH}_4$ , some other components are dissolved in the  $\text{CH}_4$  phase. The most likely dissolved component is  $\text{CO}_2$ , as  $\text{CO}_2$  is known from inclusions within emerald (Souza *et al.* 1992). However, the possibility of gases such as  $\text{N}_2$  and other hydrocarbons and volatiles cannot be ruled out, and is being tested using laser Raman and bulk chromatographic analyses.

The  $\text{CH}_4$  homogenization temperatures for those inclusions that homogenized into the vapor, liquid and critical phases may be used to calculate an estimate of methane densities using the data of Zagoruchenko & Zhuravlev (1970) for the  $\text{CH}_4$  system. The densities calculated are variable and range between 0.005 and  $0.034 \text{ g/cm}^3$ . The formation of ice or hydrate (or both) could affect the measured density of  $\text{CH}_4$  because the molar volumes of both water ice and  $\text{CH}_4$  hydrate are greater than the same mass of  $\text{H}_2\text{O}$ . The resulting contraction in the volume of the  $\text{CH}_4$  fluid phase would result in an increase in its density. This effect would shift the measured Th  $\text{CH}_4$  to higher temperatures than those in a water-free inclusion.

The temperature of initial melting, where measurable, was found to be mostly around the stable eutectic for the system  $\text{NaCl-H}_2\text{O}$ ,  $-20.8^\circ\text{C}$  (Potter & Brown 1977). These results suggest that the aqueous solutions contain mainly Na cations in solution, and belong to the system  $\text{H}_2\text{O-NaCl}$ . The exclusion of NaCl from the structure of the clathrate results in artificially high salinities in the aqueous phase of the inclusions where  $\text{CH}_4$  hydrate is present. Thus, measurement of the melting point of ice yields erroneously high values of wt.% eq. NaCl. The interpretation is further complicated by the presence of  $\text{CO}_2$  and other volatiles in the  $\text{CH}_4$  phase. Although the use of wt.% eq. NaCl in such inclusions seems inappropriate, the overestimate of the salinity based on final temperature of ice melting, with reference to the system  $\text{H}_2\text{O-NaCl}$  (Potter *et al.* 1978), ranges between 5 and 8 wt.% eq. NaCl.

Temperatures of total homogenization range from  $318^\circ$  to  $369^\circ\text{C}$  in the liquid state and from  $354^\circ$  to  $373^\circ\text{C}$  in the vapor state. Some of the measured inclusions decrepitated before total homogenization was achieved.

*Type-2 inclusions*

The complex  $\text{CO}_2 - \text{H}_2\text{O}$  inclusions show two phases at room temperature, one aqueous phase and one carbonic phase composed of  $\text{CO}_2$  vapor. During cooling, the two-phase inclusions in some cases transform into three-phase inclusions ( $\text{H}_2\text{O L} + \text{CO}_2 \text{ V} + \text{CO}_2 \text{ L}$ ). The type-2 inclusions were cooled to  $\sim -170^\circ\text{C}$ . During cooling, the aqueous liquid phase of these inclusions freezes at temperatures above  $-35^\circ\text{C}$ , and small amounts of the clathrate form around  $-45^\circ\text{C}$ ; the formation of  $\text{CO}_2 \text{ L}$  and  $\text{CO}_2 \text{ V}$  phases was observed in some inclusions, and these carbonic phases freeze at temperatures above  $-100^\circ\text{C}$ . The melting of solid  $\text{CO}_2$  has been measured to be between  $-60.8^\circ$  and  $-62.1^\circ\text{C}$ . These melting points indicate the presence of significant amounts of another component (*e.g.*,  $\text{CH}_4$ ,  $\text{N}_2$ , among others) dissolved in the  $\text{CO}_2$  phase (Hollister & Burruss 1976). It is not possible to estimate an equivalent mol. %  $\text{CH}_4$  value for these inclusions because the presence of  $\text{H}_2\text{O}$  leads to clathration.

The temperature of the first observable melting of ice is invariably above  $-20.8^\circ\text{C}$ . The salinity of the aqueous phase, expressed in terms of wt.% eq. NaCl, cannot be calculated using the melting temperatures of clathrate, because the equation of Bozzo *et al.* (1973) can be used for Tm clathrate between 0 and  $10^\circ\text{C}$ . However, salinities were overestimated approximately from the Tm ice values and the formulae proposed by Potter *et al.* (1978) for the system  $\text{H}_2\text{O-NaCl}$ , and were found to range from 5 to 10.5 wt.% eq. NaCl.

The homogenization of the  $\text{CO}_2$ -rich phases occurs between  $-11.2^\circ$  and  $10.2^\circ\text{C}$  into the vapor state, indicating that the enclosed carbonic phases have a low density ( $0.07$  and  $0.14 \text{ g/cm}^3$ ). Most of the total homogenization occurs between  $320^\circ$  and  $378^\circ\text{C}$  into the liquid state, and only two inclusions homogenized to  $381^\circ\text{C}$ , into the gas and critical state, respectively. This degree of variability in pattern of homogenization can be explained by small differences in the bulk composition of the fluid.

*Type-3 inclusions*

Temperatures of first melting of ice vary between  $-45^\circ$  and  $-55^\circ\text{C}$ ; these temperatures are lower than the eutectic temperature of the  $\text{H}_2\text{O-NaCl}$  system (Potter & Brown 1977). For this reason, the inclusions probably contain cations in solution such as  $\text{Ca}^{2+}$ ,  $\text{Mg}^{2+}$  and  $\text{K}^+$  in addition to  $\text{Na}^+$  (Crawford *et al.* 1979, Crawford 1981). The final temperature of melting of ice ranges between  $-2.1$  and  $-23^\circ\text{C}$ . Taking into account these temperatures and the experimental data of Potter *et al.* (1978) for the system  $\text{H}_2\text{O-NaCl}$ , an overestimate of the salinity ranges from 3.5 to 24.7 wt.% eq. NaCl. Homogenization temperatures range between  $160^\circ$  and  $265^\circ\text{C}$  into the liquid state. With reference to the

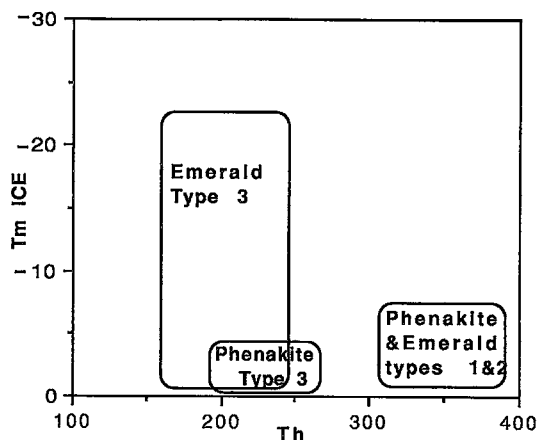


FIG. 11. Th-Tm ice diagram from Franqueira fluid inclusions. Two hydrothermal stages can be distinguished. The first hydrothermal stage was characterized by the circulation and trapping of type-1 and type-2 inclusions, circulating at minimum temperatures of between 318° and 381°C. The characteristics of type-3 inclusions, showing lower temperatures of homogenization, variable salinity, and solutions containing several cations, suggest an independent episode of fluid circulation.

T-salinity graph of Bodnar (1983), the density of the type-3 inclusions varies between 0.9 and 1.15 g/cm<sup>3</sup>.

In order to define the hydrothermal evolution of the fluids trapped in the emerald and phenakite samples of the orebody, the homogenization temperature and the temperature of final melting of ice for the three types of inclusions have been correlated (Fig. 11). In a graph of Th *versus* Tm ice, the fluid inclusions can be grouped as follows: at temperatures between 318 and 381°C, inclusions of type 1 formed in the emerald and phenakite samples, and only type-2 inclusions occurred in the core of emerald crystals, with Tm ice between -3 and -7°C; at temperatures between 160 and 265°C, type-3 inclusions occurred in the two minerals, with Tm ice data varying between -2.1 and -23°C.

From the above microthermometric data, clearly no great differences exist among the fluid inclusion populations of emerald and phenakite, and two discontinuous hydrothermal stages can be distinguished. The first hydrothermal stage was characterized by the circulation and trapping of aqueous fluid with volatiles represented by the type-1 and -2 inclusions (complex CH<sub>4</sub>-CO<sub>2</sub> aqueous inclusions), with salinities below 10 wt.% eq. NaCl, a low density of bubbles, at minimum temperatures of between 318° and 381°C. The lithostatic or hydrostatic pressure was sufficient to prevent boiling.

The fact that fluid inclusion of types 1 and 2 have high temperatures of homogenization into liquid and, less commonly, the gas and critical states, similar values in salinity, with some of them being primary and pseudosecondary in character, means that these inclusions may be considered to be contemporaneous. This suggests a stage of heterogeneous entrapment (immiscibility) in the system H<sub>2</sub>O - NaCl - CH<sub>4</sub> - CO<sub>2</sub> - other volatiles. The magmatic fluids from the pegmatite may have reacted with the host rocks or with other solutions of a different nature (metamorphic, connate or meteoric waters) to give rise to solutions trapped as fluid inclusions in the emerald and phenakite.

The characteristics of type-3 inclusions (secondary character, a lower temperature of homogenization, and lack of CH<sub>4</sub>, CO<sub>2</sub> and other volatiles, variable salinity, and presence of several cations), suggest an independent episode of circulation of hydrothermal fluid during later tectonic events. Thus, the second hydrothermal stage is considered to correspond to the circulation and trapping of aqueous solutions of salinity below 24.7 wt.% eq. NaCl, containing cations such as Ca<sup>2+</sup>, Mg<sup>2+</sup>, K<sup>+</sup> and Na<sup>+</sup>, among others, densities ranging 0.9 to 1.15 g/cm<sup>3</sup>, at minimum temperatures of trapping ranging from 160 to 265°C.

The different physicochemical characteristics found between the first stage and the second are probably due to circulation and mixing of fluids with different source (magmatic, metamorphic, connate and meteoric waters). However, to confirm this hypothesis, it will be necessary to carry out stable isotope studies.

#### COMPARISON WITH LITERATURE DATA ON FLUID INCLUSIONS IN EMERALD

There are many references to fluid-inclusion studies from various types of emerald deposits (*e.g.*, Barros & Kinnaird 1985, Barros 1986, Kupriyanova & Sokolov 1984, Mendes & Svisero 1988, Ottaway *et al.* 1986, 1994, Schwarz & Mendes 1985, Souza *et al.* 1992, Giuliani *et al.* 1995), although the results obtained are disparate owing to the different geotectonic conditions of formation. These studies show that there is a great variability in temperatures and pressures, and the inclusions may be aqueous fluids rich in CO<sub>2</sub> and other volatiles or aqueous solutions containing NaCl and other chlorides with very different salinities. In addition, isotopic studies show that the aqueous fluids associated with emerald may be predominantly meteoric, metamorphic or magmatic in origin, as well as connate waters, *e.g.*, brines derived from evaporitic sedimentary sequences. (Ottaway *et al.* 1995).

Only a few references of fluid inclusions in emerald mention the presence of CH<sub>4</sub>. This type of inclusion is important in emerald of the Franqueira ore and distinguishes these crystals of emerald from the other emerald ores in the world. Nevertheless, the fluid-

inclusion studies of Brazilian emerald (Souza *et al.* 1992) show that from a morphological point of view (tube-like, canal-shaped, and geometric cavities), the emerald crystals of Franqueira and Brazil are similar.

#### GENETIC MODEL

In order to explain the genesis of this type of deposit, the possible origin of each one of the different rocks will be discussed.

The presence in the northwestern sector of the Iberian Peninsula of the Ordenes, Braganza and Morais complexes, all of which are overthrust, ophiolitic (Barrera *et al.* 1989) and dunite-bearing, leads us to propose that the dunite and hornblende gabbro considered here belong to a remnant of peridotitic and gabbroic rocks from the overthrust complexes. The compositional characteristics of the spinel, olivine and titanian clinohumite analyzed with the electron microprobe (Figs. 6–8), coincide with those analyzed by Monterrubio (1991) in the Ordenes and the Cabo Ortegal Complexes, and the olivine is typical of alpine peridotite. Later, during the intrusion of the Hercynian granites, the dunite and hornblende gabbro could have remained in the roof zone of the peraluminous hetero-

geneous two-mica granites, which normally have a suite of associated pegmatite bodies.

These pegmatites, in contact with the dunite and Be-, B- and P-rich fluids, caused metasomatic adjustments, with the corresponding transformation of the dunite to phlogopite and tremolite near the pegmatite bodies (Fig. 12). In the zones closest to the pegmatite, the dunitic rock was transformed entirely (in response to water, Si, Al and K from the pegmatite) into a rock made up for the most part of phlogopite. In the zones farthest from the pegmatite, where only Si and H<sub>2</sub>O were introduced from the pegmatite, the dunite was transformed into tremolite. Close to the dunite, orthoamphibole (anthophyllite) was formed. The Mg and Cr of these rocks were provided by the dunite.

The addition of boron and P formed tourmaline and abundant apatite in the metasomatic facies, with phlogopite. In the zones closest to the pegmatite, the Be spreads out in the system and first developed chrysoberyl ("alexandrite") and phenakite porphyroblasts, isolated or both intergrown in the phlogopite. Subsequently, beryl porphyroblasts developed and partially replaced the other two Be minerals. Invariably, where chrysoberyl and phenakite are

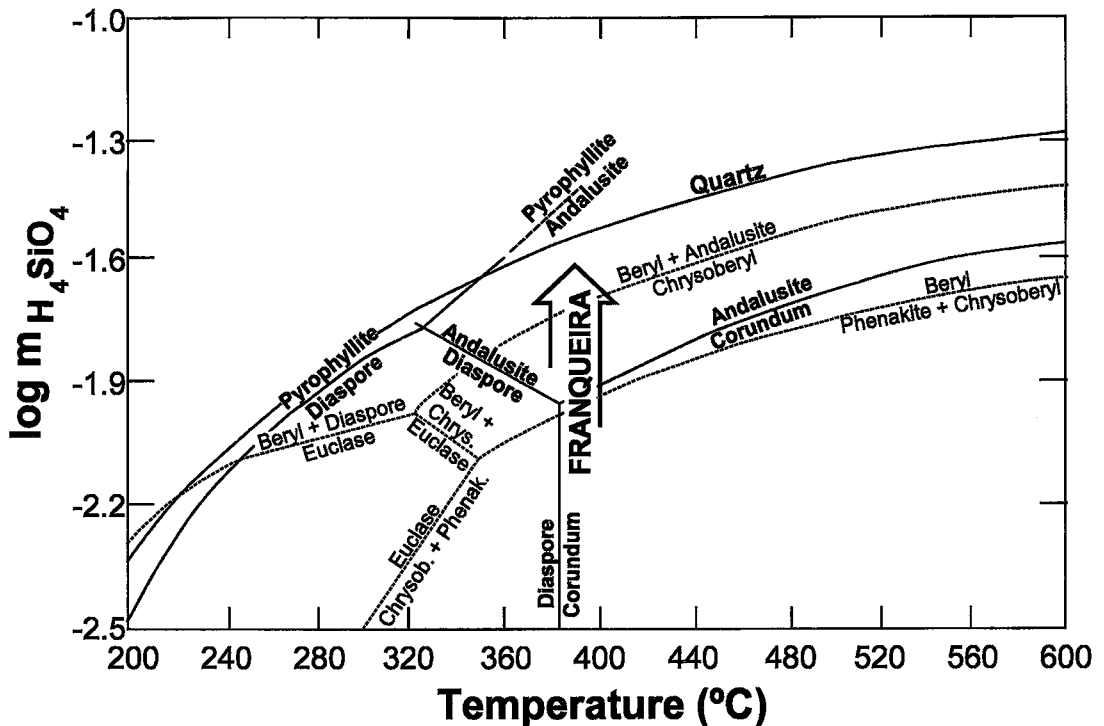


FIG. 12. Log  $m_{H_4SiO_4}$  - temperature projection at  $P = 1$  kbar and activity of beryl = 0.1, showing a path consistent with the evolution of Be assemblages at Franqueira.

# EXOMETASOMATISM

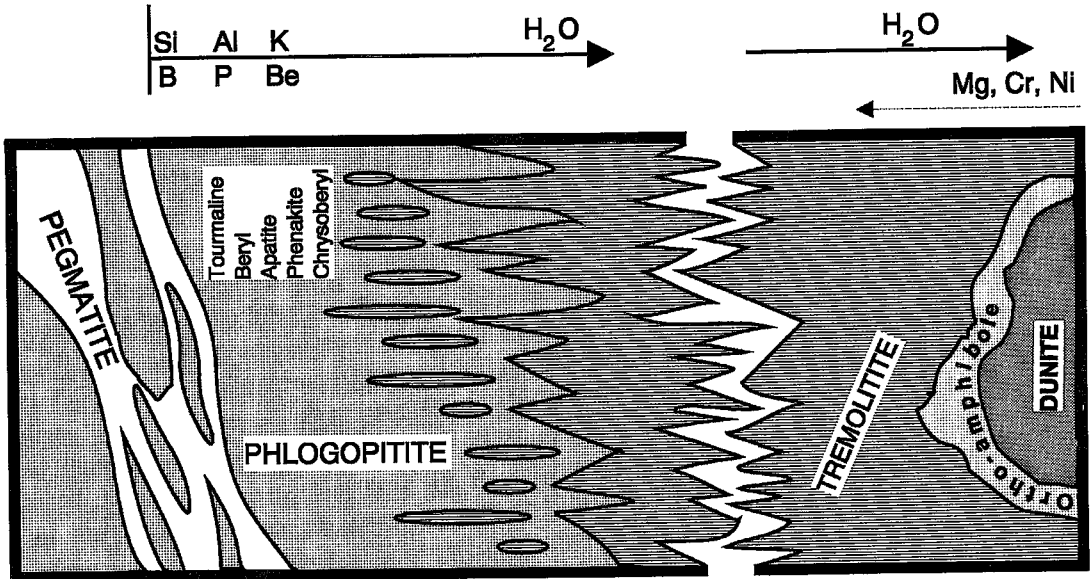


FIG. 13. Schematic genetic model of the Franqueira gemstone deposit.

together, they are replaced by beryl and appear as a skeletal intergrowth within the emerald. The fact that chrysoberyl formed early is probably due to the fact that this mineral and olivine have the same type of crystal structure; therefore, the growth of chrysoberyl could be favored by a decrease in the energy threshold necessary for epitaxial nucleation on olivine relics during the phlogopitization of the dunite, always with the appropriate activity of Si. The presence of orthoamphibole inclusions in emerald crystals could represent olivine, which is transformed owing to the presence of H<sub>2</sub>O.

A thermodynamic approach to the evolution of the beryllium mineralization of Franqueira can be made on the basis of the equilibrium model in the BeO–Al<sub>2</sub>O<sub>3</sub>–SiO<sub>2</sub>–H<sub>2</sub>O system developed by Barton (1986). Fluid-inclusion data give us temperatures of formation much lower than those corresponding to the stability field of chrysoberyl + quartz, and close to the euclase = beryl + phenakite + chrysoberyl join. The absence of euclase indicates a minimum range of temperatures and pressures, corresponding to a P of 4 kbars and a T ranging from approximately 350°C (for P = 1 bar) to about 450°C (for P = 4 kbars), in the stability field of andalusite. The pressure in the system must have been, in fact, much lower than 4 kbars, because the mineralization is formed as a result of contact metamorphic – metasomatic processes. Pressures in the order of 1–2 kbars and temperatures of

about 380–420°C are proposed, which are consistent with the fluid-inclusion data.

Some of the emerald crystals could have formed according to the reaction beryl = phenakite + chrysoberyl + quartz (Barton 1986), until the exhaustion of quartz. Skeletal remains of phenakite and chrysoberyl appear in emerald crystals. In the bulk of the phlogopitite, there is no quartz. Only two small remnants of quartz (20 and 10 µm) included in one emerald crystal were observed. However, these considerations must be evaluated with care, because the results of Barton (1986) for this reaction were obtained in dry experiments with pure quartz and Be-minerals, and in relation to the stability fields of the Al<sub>2</sub>SiO<sub>5</sub> polymorphs with the assumption that aluminum is relatively immobile. At Franqueira, the mineralization consists essentially of phlogopite, and most of the Si and Al present in the system are involved in its formation. The evolution of the mineralization appears to be controlled by the addition of water, silica, alumina and Be to the system, in nonequilibrium conditions. The role of minor elements present in phlogopite and Be-minerals in relation to the stabilization of these phases also cannot be neglected. The content of alkali metals in the emerald suggests an activity of beryl clearly lower than 1.

It is evident that in the Franqueira deposit, Be oxides are replaced by Be silicates. This implies increasing activity of silica assuming a negligible decrease in

temperature during the two main stages of mineralization, as can be inferred from fluid-inclusion data. A projection in terms of silica activity (as  $\log m_{\text{H}_4\text{SiO}_4}$ ) – temperature showing a path consistent with this assumption can be seen in Figure 12. A  $\log m_{\text{H}_4\text{SiO}_4}$  ranging between -1.6 and -2.0 is inferred for the assemblage present at Franqueira, assuming a total pressure of 1 kbar and an activity of beryl equal to 0.1.

Thus, the model proposed (Fig. 13) to explain the genesis of the Franqueira gemstone deposit is based on a metasomatic interaction between dunite and granitic pegmatite. Between both rocks, a zone of chemical interchange is established in which the most important contribution is from the pegmatite to the dunite (exometasomatism), whereas the contribution from the dunite to the pegmatite is not important. According to the fluid-inclusion data, the fluid involved was complex in the system  $\text{H}_2\text{O}-\text{NaCl}-\text{CO}_2-\text{CH}_4$  – “other volatile”. The formation of the beryllium minerals took place around 400°C from a heterogeneous fluid (undergoing immiscibility) trapped as type-1 and -2 fluid inclusions. The characteristics of type-3 inclusions suggest an independent episode of fluid circulation owing to the development of hydrothermal cells during later tectonic events.

The conditions of geological formation of the Franqueira deposit lead us to include it in the Suture Zone group (Snee & Kazmi 1989), in which the Cr-rich mafic rocks were overthrust onto continental crust and subsequently cross-cut by Be-rich granitic pegmatite. This is the first cited locality in the Hercynian belt with the association of emerald, chrysoberyl and phenakite. The presence, in the Galicia – Tras os Montes zone of the Iberian Massif, of a number of ophiolite overthrust complexes that are cross-cut by pegmatite-bearing granites, some of them rich in beryllium minerals, gives it special interest as a potential source of emerald and chrysoberyl (“alexandrite”). The Franqueira ore increases the interest of the zone for prospection of new ores with the same characteristics.

#### ACKNOWLEDGEMENTS

The authors express their gratitude to D.J.R. García for the samples containing chrysoberyl and Jose Mangas, of Las Palmas University, for his help with fluid inclusions. This work has been financed by the CICYT, project GEO 91/1077 and Oviedo University project df91/21527. We thank the reviewers and editor for their encouraging suggestions, which have improved significantly the content and clarity of the paper.

#### REFERENCES

- BARRERA, J., FARIAS, P., LODEIRO, F., MARQUINEZ, J., MARTIN-PARRA, L., MARTINEZ CATALAN, J., OLMO, A. & PABLO, J.G. (1989): Mem Mapa Geol España E 1:200.000 Ourense. Inst. Tecnológico Geominero de España, Madrid, 284 p.
- BARROS, J.C. (1986): Fluid inclusions, genetic models and exploration strategies for emerald deposits: cases from Brazil. *Terra Cognita* **6**(3), 509 (abstr.).
- & KINNAIRD, J.A. (1985): Fluid inclusion studies of emeralds and green beryls from the Porangatu deposit, Goiás State, Brazil. Fluid Inclusions 8th Symp. (Göttingen), 8-9 (abstr.).
- BARTON, M.D. (1986): Phase equilibria and thermodynamic properties of minerals in the  $\text{BeO}-\text{Al}_2\text{O}_3-\text{SiO}_2-\text{H}_2\text{O}$  (BASH) system, with petrologic applications. *Am. Mineral.* **71**, 277-300.
- BODNAR, R.J. (1983): A method of calculating fluid-inclusion volumes based on vapor bubble diameters and P-V-T-X properties of inclusion fluids. *Econ. Geol.* **78**, 535-542.
- BOZZO, A.T., CHEN, HSIAO-SHENG, KASS, H.J. & BARDUHN, A.J. (1973): The properties of the hydrates of chlorine and carbon dioxide. In Fourth Int. Symp. on Fresh Water from the Sea (A. Delyannis & E. Delyannis, eds.), **3**, 437-451.
- BURRUSS, R.C. (1981): Analysis of phase equilibria in C-O-H-S fluid inclusions. In Fluid Inclusions: Applications to Petrology (L.S. Hollister & M.L. Crawford, eds.). *Mineral. Assoc. Can., Short-Course Handbook* **6**, 39-74.
- COLLINS, P.L.F. (1979): Gas-hydrates in  $\text{CO}_2$  bearing fluid inclusions and the use of freezing data for estimation of salinity. *Econ. Geol.* **74**, 1435-1444.
- CRAWFORD, M.L. (1981): Phase equilibria in aqueous fluid inclusions. In Fluid Inclusions: Applications to Petrology (L.S. Hollister & M.L. Crawford, eds.). *Mineral. Assoc. Can., Short-Course Handbook* **6**, 75-100.
- , FILER, J. & WOOD, C. (1979): Saline fluid inclusions associated with retrograde metamorphism. *Bull. Minéral.* **102**, 562-568.
- FERSMAN, A.E. (1929): Geochemische Migration der Elemente. III. Smaragdgruben im Uralgebirge Abhandlungen zur praktischen Geologie und Bergwirtscha. Ed. Wilhelm Knapp, Halle (Saale) **1**, 74-116.
- GASPAR, J.C. (1992): Titanian clinohumite in the carbonatites of the Jacupiranga Complex, Brazil: mineral chemistry and comparison with titanian clinohumite from other environments. *Am. Mineral.* **77**, 168-178.
- GIULIANI, G., CHEILLETZ, A., ARBOLEDA, C., CARRILLO, V., RUEDA, F. & BAKER, J. (1995): An evaporitic origin of the parent brines of Colombian emeralds: fluid inclusion and sulphur isotope evidence. *Eur. J. Mineral.* **7**, 151-165.
- , SILVA, L.J.H.D. & COUTO, P. (1990): Origin of emerald deposits of Brazil. *Mineral. Deposita* **25**, 57-64.
- HOLLISTER, L.S. & BURRUSS, R.C. (1976): Phase equilibria in fluid inclusions from the Khtada Lake metamorphic complex. *Geochim. Cosmochim. Acta* **40**, 163-175.

- JAN, Q.M. & WINDLEY, B.F. (1990): Chromian spinel – silicate chemistry in ultramafic rocks of the Jijal complex, northwest Pakistan. *J. Petrol.* **31**, 667-715.
- KRETZ, R. (1983): Symbols for rock-forming minerals. *Am. Mineral.* **68**, 277-279.
- KUPRIYANOVA, I.I. & SOKOLOV, S.V. (1984): The conditions of formation of phlogopite – margarite – beryl mineralization. *Int. Geol. Rev.* **27**, 306-318.
- LAZNICKA, P. (1985): *Empirical Metallogeny: Depositional Environments, Lithological Associations and Local Metallic Ores*. Elsevier, Amsterdam, The Netherlands.
- LEAKE, B.E. (1978): Nomenclature of amphiboles. *Am. Mineral.* **63**, 1023-1052.
- MATTE, P.H. (1968): La structure de la virgation hercynienne de Galicia (Espagne). *Trav. Lab. Geol. Fac. Sci. Grenoble, Revue de Géol. Alpine* **44**, 1-128.
- MENDES, J.C. & SVISERO, D.P. (1988): Solid and fluid inclusions in Santa Teresinha de Goias emeralds and its geological significance. *Anais XXXV Congresso Brasileiro de Geol. (Belem, Brazil)* **1**, 398-405.
- MIDDLEMOST, E.A.K. (1985): *Magmas and Magmatic Rocks*. Longman, London, U.K.
- MONTEERRUBIO, S. (1991): *Mineralizaciones asociadas a rocas ultrabásicas en el hercínico español*. Tesis Doctoral, Univ. Complutense de Madrid, Madrid, Spain.
- OTTAWAY, T.L., WICKS, F.J., BRYNDZIA, L.T., KYSER, T.K. & SPOONER, E.T.C. (1994): Formation of the Muzo hydrothermal emerald deposit in Colombia. *Nature* **369**(6481), 552-554.
- \_\_\_\_\_, \_\_\_\_\_, \_\_\_\_\_ & SPOONER, E.T.C. (1986): Characteristics and origin of the Muzo emerald deposit, Colombia. *Int. Mineral. Assoc., Abstr.*, 193.
- POTTER, R.W., II & BROWN, D.L. (1977): The volumetric properties of aqueous sodium chloride solutions from 0° to 500°C at pressures up to 2000 bars based on a regression of available data in the literature. *U.S. Geol. Surv., Bull.* **1421-C**, 1-36.
- \_\_\_\_\_, CLYNNE, M.A. & BROWN, D.L. (1978): Freezing point depression of aqueous sodium chloride solutions. *Econ. Geol.* **73**, 284-285.
- POTY, B., LEROY, J. & JACHIMOWICZ, L. (1976): Un nouvel appareil pour la mesure des températures sous le microscope; l'installation de microthermométrie Chaixmeca. *Bull. Soc. Franç. Minéral. Cristallogr.* **99**, 182-186.
- ROEDDER, E. (1962): Studies of fluid inclusions. I. Low temperature application of a dual-purpose freezing and heating stage. *Econ. Geol.* **57**, 1045-1061.
- \_\_\_\_\_ (1984). Fluid Inclusions. *Rev. Mineral.* **12**.
- SCAMBELLURI, M., STILATING, E.E.H., PICCARDO, G.B., VISSERS, R.L.M. & RAMPONE, E. (1991): Alpine olivine- and titanian clinohumite-bearing assemblages in the Erto-Tobbio peridotite (Voltri Massif, NW Italy). *J. Metamorphic Geol.* **9**, 79-91.
- SCHWARZ, D. & MENDES, J.C. (1985): Estudo comparativo das inclusões nas esmeraldas de Itabira/MG e Santa Teresinha/GO. In *Simp. Geol. Minas Gerais, Brazil* **5**, 154-164.
- SINKANKAS, J. (1989): *Emerald and other Beryls*. Geoscience Press, Prescott, Arizona.
- SOUZA, J.L., MENDES, J.C., SILVEIRA BELLO, R.M., SVISERO, D.P. & VALARELLI, J.V. (1992): Petrographic and microthermometrical studies of emeralds in the Garimpo of Capoeirana, Nova Era, Minas Gerais State, Brazil. *Mineral. Deposita* **27**, 161-168.
- SNEE, L.W. & KAZMI, A.H. (1989): Origin and classification of Pakistani and world emerald deposits. In *Emeralds of Pakistan, Geology, Gemology and Genesis* (A.H. Kazmi & L.W. Snee, eds.). Van Nostrand Reinhold Co., New York, N.Y. (230-236).
- VLASOV, K.A. & KUTAKOVA, E.I. (1960): *Emerald Deposits*. Akademiya Nauk SSSR, Moscow, Russia (in Russ., cited in Sinkankas 1989).
- ZAGORUCHENKO, V.A. & ZHURAVLEV, A.M. (1970): *Thermophysical Properties of Gaseous and Liquid Methane*. Israel Program Sci. Translations, Jerusalem, Israel.

Received March 7, 1994, revised manuscript accepted January 7, 1995.

APPENDIX:  
ANALYTICAL TECHNIQUES

The mineralogical study of this rock has been made using transmitted and reflected-light polarizing microscopes, refractometers, electron microprobe (with international standards) and scanning electron microscopy. For mineral identification, we also used X-ray powder diffraction, especially for fluorapatite, emerald, phenakite and chrysoberyl. The Philips PW 1729/1710 diffractometer was used with  $\text{CuK}\alpha$  radiation at 40 kV and 30 nA.

Whole-rock and trace-element analyses were performed in Canada at ACME Analytical Laboratories Ltd. Concentrations of  $\text{SiO}_2$ ,  $\text{Al}_2\text{O}_3$ ,  $\text{Fe}_2\text{O}_3$  (as total iron),  $\text{MgO}$ ,  $\text{CaO}$ ,  $\text{Na}_2\text{O}$ ,  $\text{K}_2\text{O}$ ,  $\text{TiO}_2$ ,  $\text{P}_2\text{O}_5$ ,  $\text{MnO}$ ,  $\text{Cr}_2\text{O}_3$ , LOI, Ba, Sr, Zr, Y were established by ICP. Samples (0.2 g) are fused with 1.2 g of  $\text{LiBO}_2$  and are dissolved in 100 mL 5%  $\text{HNO}_3$ . The detection limits are, for all oxides 0.01%, for Sr and Y, 10 ppm, for Zr, 20 ppm, for Ba, 5 ppm. Concentrations of As, Ni, Cu, Co, Be, Li and La were established by ICP. Samples (0.5 g) were digested with 3 mL 3–1–2  $\text{HCl-HNO}_3\text{-H}_2\text{O}$  at 95°C for one hour and were diluted to 10 mL with water. The detection limits are: As, Ni, Cu, Co, Li, La 2 ppm, Be 0.2 ppm. Sample preparation was performed at the University of Oviedo. Five kg of rock were reduced to 3–4 mm by crushing, and 100 g were pulverized to at least 150 mesh in a mild steel to minimize Cr contamination.

The most important minerals were analyzed with a CAMEBAX SX50 electron microprobe. In all cases, the standard deviation of results is less than 5%. Concentrations of the light elements have been calculated by stoichiometry. Electron-microprobe analyses were performed at the University of Oviedo. The beam conditions were 15 kV and 15 nA; the data were ZAF-corrected. The following international standards were used: ALB1, ORTH, ALB1, FE2O, MNTI, ANDO, MGO, CR2O, MNTI, NIO. The detection limits were 0.03 wt.% for Ni, Mn; 0.02% for Fe, Cr, Ti, Al, and 0.01% for the others.

Microthermometric studies of fluid inclusions were performed on 300- $\mu\text{m}$  thick plates using a microscope equipped with a UMK50 Leitz objective and a

Chaixmeca cooling and heating stage (Poty *et al.* 1976) in the Laboratory of Geology of the University of Las Palmas (Spain). The stage was calibrated according to the procedures outlined by Poty *et al.* (1976). Most populations of fluid inclusions could not be distinguished on the basis of room temperature (22 to 25°C) observations. Most inclusions were cooled below  $-140^\circ\text{C}$ , in order to check for low-temperature phase changes. In all cases, freezing measurements were completed before the inclusions were heated above 25°C. The following phase-transition temperatures have been measured: Tn ice, Tn hyd  $\text{CH}_4$ , Tn clath, Tn  $\text{CO}_2$ , Tm  $\text{CO}_2$ , Th  $\text{CH}_4$ , Th  $\text{CO}_2$ , Te ice, Tm ice, Tm hyd, Tm clath and Th [microthermometric abbreviations after Roedder (1984)]. Estimates of the precision of individual measurements were made by repeating inclusion runs. Precision varied from  $\pm 0.1^\circ\text{C}$  for Tm to  $\pm 2^\circ\text{C}$  for Th. The dark borders of the cavities, high volumetric ratios and small sizes of some inclusions makes microthermometry difficult, particularly in the measurements of Th  $\text{CO}_2$ , Th  $\text{CH}_4$  and Th data.

Gas hydrate was detected in the inclusions by the presence of a double freezing event during cooling (hydrate and ice; Collins 1979). However, as only amounts of hydrate formed, it was impossible to observe hydrate melting directly. In order to determine the melting temperature of the hydrate as accurately as possible, a freeze/refreeze technique was used (Roedder 1962). This technique involves raising the temperature of the inclusion to a fixed point (*e.g.*,  $10^\circ\text{C}$ ) and then freezing it again rapidly. If any solid clathrate remains in the inclusion, a solid phase will grow back immediately on cooling, resulting in shrinkage and "squashing" of the vapor bubble. When a temperature is reached at which no further deformation of the vapor bubble occurs on quenching, then the hydrate has melted. Using this technique, hydrate measurements were made with a precision of  $\pm 0.5^\circ\text{C}$ . As will become clear from the salinity calculations, it is necessary to determine the melting point of the hydrate as precisely as possible.